Wetlands
DOI 10.1007/s13157-014-0534-1

ARTICLE

Hydrological and Geomorphological Controls on the Water Balance Components of a Mangrove Forest During the Dry Season in the Pacific Coast of Nicaragua

Heyddy Calderon · Ruben Weeda · Stefan Uhlenbrook

Received: 20 December 2013 / Accepted: 3 April 2014

Abstract Hydrological and geomorphological processes are key to mangrove forest growth and development. However, few mangrove hydrology studies exist in Central America. A 0.2 km^2 mangrove forest on the Pacific coast of Nicaragua was investigated to determine the water balance dynamics during the dry season. The used multi-methods approach combined hydrology, hydrochemistry and geophysics. Precipitation is the main freshwater input. Beach ridges are the key geomorphologic features which allowed an increase in water storage of 351 m^3d^{-1} during a 22 day period. Large precipitation events cause breaking of the beach ridges by excess water, suddenly emptying the system. Grey water and pit latrines from the nearby town influence shallow groundwater quality, but also provide extra nutrients for the mangrove forest. Groundwater chemistry is also affected by calcite dissolution and seawater. Refreshening and salinization processes are controlled by the general groundwater flow direction. Hydraulic and hydrochemical influence of seawater on coastal piezometers seems to be controlled by the elevation of the water table and the tidal amplitude. These conditions control forest subsistence during the dry season, which is essential for the mangrove forest to provide ecological and economic benefits such as protection against flooding, habitat for numerous species, and tourist attraction.

Keywords Mangrove forest · Water balance · Geomorphology · Hydrochemistry · Nicaragua

H. Calderon (✉) · S. Uhlenbrook
Department of Water Science and Engineering, UNESCO-IHE, Delft3015, 2601, DA, Netherlands
e-mail: h.calderonpalma@unesco-ihe.org

H. Calderon
Nicaraguan Aquatic Resources Research Center at the National Autonomous University of Nicaragua (CIRA-UNAN), P.O. Box 4598 Managua, Nicaragua

R. Weeda
VU Amsterdam, Department of Hydrology, Amsterdam 1081 HV, Netherlands

S. Uhlenbrook
Delft University of Technology, Section of Water Resources, DelftP.O. Box 5048, 2600, GA, Netherlands

Introduction

Wetlands are at the interface between aquatic and terrestrial ecosystems. Wetlands in coastal areas in equatorial regions form mangrove swamps, whereas at higher latitudes they tend to form salt marshes (Keddy 2010). Mangroves can be very broadly defined as an assemblage of plants all adapted to a wet, saline habitat (Thom 1967; Feller and Sitnik 1996). Increased water level caused by climate change is one the many threats to mangrove forest survival worldwide (Alongi 2002; Gilman et al. 2008; Polidoro et al. 2010; Briceño et al. 2013).

Mangrove forests are usually located between mean sea level and the highest spring tide with different mangrove tree species typically occurring in zones parallel to the coast (Alongi 2002). This zonation is attributed to salinity, soil type and chemistry, nutrient content, physiological tolerances, predation and competition (Smith et al. 1992). Thom (1967) established that the most important factors controlling mangrove zonation are substratum and water flow regime. Preservation of dynamic flow regimes is critical to maintain riverine ecosystems (McClain et al. 2013) like mangrove forests. Therefore, knowledge of hydrological and geomorphological processes in mangrove forests are critical for understanding the functioning, as well as conservation, protection, and sustainable management, of these fragile ecosystems.

Published online: 01 May 2014

According to Ellison (2004), wetlands in Central America, including mangrove forests, cover approximately 40,000 km^2 (8% of the total area). However, the exact extent and health of mangroves is not known since ecological studies have been focused on Costa Rica and Panama wetlands (Ellison 2004). Groombridge (1992) estimated between 6,500 km^2 and 12,000 km^2, while Spalding et al. (1997) estimated between 8,000 km^2 and 9,000 km^2, excluding Belize. On the Atlantic coast, mangroves form narrow bands along the coastal plains, whereas on the Pacific coast mangroves extend further inland with extensive forests in major river deltas such as the Estero Real in Nicaragua (Ellison 2004). There are approximately 4,000 km^2 of mangrove forests on the Pacific coast of Central America (Jimenez 1992). Ellison (2004) estimated that there are 2,000 km^2 of mangrove forests on the Atlantic coast of Nicaragua, but only 400 km^2 on the Pacific Coastside.

Dry climate mangroves are found on the Pacific Coast where precipitation is below 1,800 mm year^{-1} distributed mainly between May and November as opposed to the more than 2,000 mm year^{-1} at the Atlantic side. Soil salinity increases inland as the influence of tidal flooding is reduced, and salt accumulation is enhanced by evaporation. In this kind of environment, evaporation and freshwater inputs impact growing conditions, species composition, and structural development, thus increasing variability of forest composition from site to site (Jimenez 1992). Freshwater flows also equilibrate nutrient inputs which affects the food web within the mangroves (Briceño et al. 2013). Understanding of sources of freshwater inputs into mangrove ecosystems is vital for their conservation and protection (Gondwe et al. 2010).

Most of the literature on mangroves in Central America is related to biological (Schumacher 2007; Gross et al. 2013), ecological (Pool et al. 1977; Rabinowitz 1978; Roth 1992; Carvalho et al. 1999; Cahoon et al. 2003; Ellison 2004; Lovelock et al. 2004; Gross et al. 2013) and socioeconomic characteristiscs (Fürst et al. 2000). Few studies were found on the relationship of mangrove forests and hydrology. A study in the dry life zone of the Gulf of Honduras investigated mangrove zonation patterns finding a great influence of soil salinity (Castañeda-Moya et al. 2006). Another study in Costa Rica used the water balance to study *Avicennia bicolor* in a dry weather zone, finding a great influence of rainfall and runoff on the structure and function of the forest (Jimenez 1990).

There are few studies on mangroves in Nicaragua (Carvalho et al. 1999; Fürst et al. 2000; Schumacher 2007; Perez et al. 2008). Nevertheless, they address exclusively the ecological and economic value of large mangrove forests. No references were found regarding the hydrological functioning of this type of ecosystem in Nicaragua; even though the water flow regime is recognized as one of the most important factors controlling mangrove forest structure and functioning (Thom 1967). Moreover, the hydrological cycle may influence biogechemical processes within mangrove forest soils (Sherman et al. 1998).

An example of a small, unstudied mangrove ecosystem was found in the southwestern coast of Nicaragua, south of the city of San Juan del Sur, near the town of Ostional (Fig. 1). The estuarine mangrove forest occurs along the floodplain of the river Ostional. This small forest has an approximate area of 0.2 km^2, yet provides valuable economic and ecological services in terms of tourist attraction, protects the area against flooding, and provides habitat for numerous species. This mangrove forest is part of the biological corridor of the Pacific of Nicaragua, providing biological interconnectivity with other ecosystems (CBM 2002). The beaches of the area are nesting sites for an endangered sea turtle species, *Lepidochelys olivacea*.

The objective of this study was to determine the water balance dynamics of a mangrove forest during a dry period. The research focused on (i) determining the sources and fluxes of freshwater which influence mangrove subsistence during the dry season using hydrological, hydrochemical and geophysical methods, and (ii) identifying geomorphological and hydrological controls on the water balance components.

Study Area

General

The town of Ostional is a rural community located on the Pacific Coast of southwestern Nicaragua. It has an estimated population of 1,500 people. There is a water supply system which relies on a single 60 m deep well, which suffers from constant malfunctioning, forcing the population to use shallow hand dug wells. There is no sewage treatment system but there are about 100 pit latrines, with most (70) in poor sanitary and structural condition. Of 90 septic tanks, 30 are defective and leak (Weeda 2011); grey water, generated from laundry, showers and kitchens, is directly discharged to the ground. Agriculture and fishing are the main economic activities in the area. The town is located at the flood plain of the Ostional River, and according to the National System of Disaster Prevention (SINAPRED) is prone to flooding during high precipitation season (September–October) (SINAPRED 2005). Land use is dominated by forest (52 %), agriculture (20 %) and pasture (28 %) (UNA 2003).

Regional Geology

The study area is located in the geologic province of the Pacific rim, within the Rivas-Tamarindo sub-province. This environment originated from deposition of sediments during processes of sea transgression and regression. Volcanic activity also contributed to the formation of this sub-province.

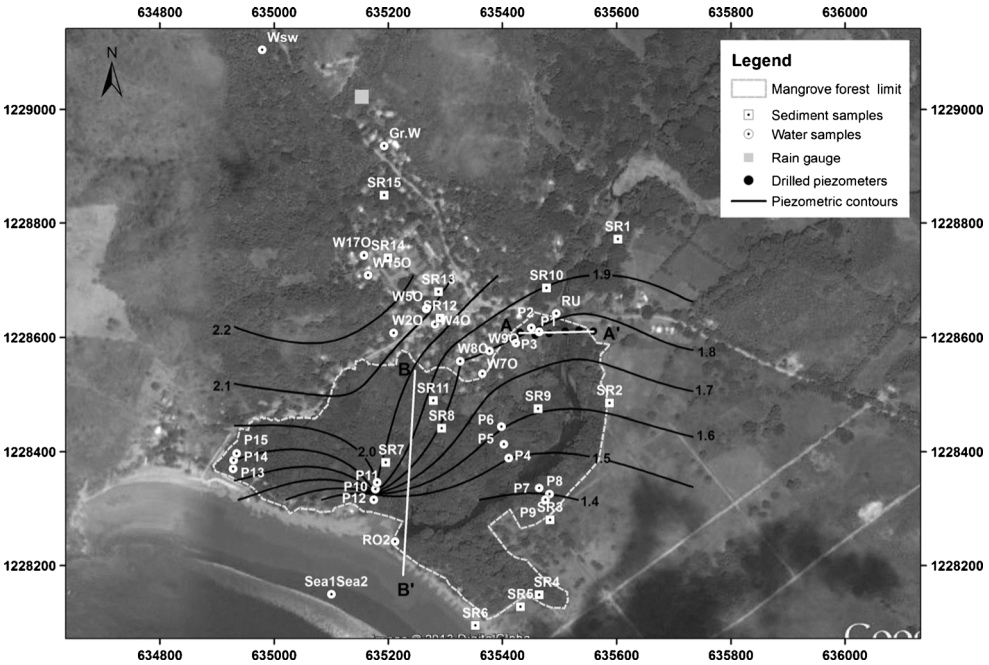

Fig. 1 Location of study area depicting the average piezometric surface of shallow groundwater in the study period as well as cross sections A–A and B–B

Tectonic activities in this subduction zone (the contact of the Caribbean and Cocos Plates), caused compression forces which formed the Rivas Anticline, oriented from the NW to the SE. The Upper Cretaceous Rivas Formation is exposed in the large Rivas anticline along the southwestern part of Lake Nicaragua and consists of about 2,700 m of tuffaceous shale and sandstone. The Rivas Formation is overlain by the 2,750 m thick Paleocene-Eocene Brito Formation. The Brito Formation is exposed west and north of the Rivas anticline and is comprised of volcanic breccias, tuffs, shales, sandstone and limestone. The compressional forces responsible for the formation of the anticline also caused faulting and fracturing of these two formations creating a fracture system parallel to the ridge of the anticline (Swain 1966; Krasny and Hecht 1998). Only the Brito Formation is exposed in the study area.

Climate, Hydrology and Hydrogeology

According to the Koppen climate classification, the climate is tropical wet and dry (Aw). The rainy season starts in May and ends in November, with September and October being the wettest months with an average of 215 mm month^{-1} and 267 mm month^{-1}, respectively. During July and August there is generally a 3 to 5 week period of no precipitation known as the midsummer drought (Magaña et al. 1999). Historical climatic data for the period 1965–2007 from the nearest station located in Rivas (40 km NW from Ostional) indicates a mean temperature of 27.1 °C. Wind direction is predominantly towards the East with an average wind velocity of 5 m s^{-1}. Mean annual precipitation is 1476 mm year^{-1} and mean pan evaporation amounts to 1976 mm year^{-1}.

The upstream catchment area is characterized by exposed fractured shale and intermittent streams with sandstone streambeds. Downstream, alluvial deposits of unknown thickness are found. River discharge varies between 0.1 m^3 s^{-1} (March) and 13 m^3 s^{-1} (October) (CIRA 2008). The aquifers found in the area are formed by weathering and faulting or fracturing of sedimentary rocks, partially filled by alluvial deposits. Transmissivity values, which is a measure of the amount of water that can be transmitted horizontally through a unit width of the total saturated thickness of the aquifer under a hydraulic gradient of 1 (Fetter 2001), are less than 500 m^2 d^{-1} (Krasny and Hecht 1998). The thickness of the weathered zone where aquifers might form is not known. Alluvial deposits are found in the valleys. Nonetheless, it is believed that these deposits are only a few meters thick (Krasny and Hecht 1998). According to the regional hydrochemical map, groundwater types found the area of Ostional vary between HCO_3–Ca and HCO_3–Ca–Mg.

Methods

Soil and Water Sampling

Soil samples were collected at fifteen locations in the study area (Fig. 1) at 0.25 m depth intervals up to a maximum depth of 3 m. Grain size analyses were conducted using laser diffraction performed by a FRITSCH laser particle sizer A22. Grain size was used to determine soil type according to the USDA textural classification. Cation exchange capacity (CEC) was estimated according to Appelo and Postma (1993).

Shallow groundwater and surface water samples were collected from the river upstream of the mangrove forest (RU) and at the river outlet during high (RO1) and low tide (RO2). Sea1 and Sea2 samples correspond to high and low tide, respectively. Groundwater was sampled at eight excavated shallow wells (W), one deep (60 m) well (Wsw), and from six piezometers (P; depths 1.8–3 m). Locations are shown in Fig. 1. Electrical conductivity (EC), temperature, pH and alkalinity (HCO_3^-) were determined *in situ*. Samples were filtered through a 0.45 μm glass microfiber filter. Samples for cation analyses were acidified with concentrated H_2NO_3 to prevent precipitation reactions and cation attachment to the surface of the sample bottle.

Major cations (Mg^{2+}, Ca^{2+}, Mn^{2+}, NH_4^+, Fe^{2+}) were analyzed using an Inductively Coupled Plasma-Optical Emission Spectrometer (ICP–OES: Perkin Elmer Optima 3000), while Na^+ and K^+ were measured using a flame Atomic Emission Spectroscope (AES: Perkin Elmer AAnalyst 200). The major anions (Cl^-, HCO_3^-, SO_4^{2-}, NO_3^{2-}) were measured using an Ion Chromatography System (IC: Dionex ICS 1000). The calculated ion balance error was between −10 % and +10 %, samples with higher errors were discarded. Analyses were performed at UNESCO-IHE laboratories in Delft, The Netherlands.

Hydrochemistry results were examined using a Piper diagram and the fraction of seawater (f_{sea}) based on Cl^- concentration according to Eq. 1 from Appelo and Postma (1993):

$$f_{sea} = \frac{m_{Cl^-,sample} - m_{Cl^-,fresh}}{m_{Cl^-,sea} - m_{Cl^-,fresh}} \quad (1)$$

where m is chloride concentration for the sample, the freshwater end-member and the seawater end-member. Concentration for freshwater was taken from sample Wsw, a deep well located outside the town (Fig. 1). Concentration for seawater corresponds to sample Sea1.

Ion correlations between Ca^{2+}, Mg^{2+}, Na^+, K^+, SO_4^{2-}, and Cl^- were also examined. This is a group of ions that can be considered to behave as conservative tracers in the salinization process (Giménez and Morell 1997; Ghiglieri et al. 2012).

Stratigraphy and Geophysics

Fifteen shallow piezometers were installed by hand auger drilling within the mangrove forest (Fig. 1). A PVC pipe of 0.0254 m diameter was used for the piezometers. Elevations were obtained from a GPS Garmin 62sc, which was calibrated with a local topographic benchmark.

Percussion and rotation drillling was performed to install six deeper piezometers at a cross section of the river (A–A in Fig. 1). Percussion drilling is a technique whereby a drill bit is hammered into the ground, rotary drilling uses a rotating drilling bit. Piezometers depths vary between 5 and 25 m, with depth increasing away from the river on the West and East sides (Fig. 2). Percussion drilling was used for the first 10–15 m where relatively soft materials were encountered. Split spoon samples were collected every 0.7 m, providing undisturbed samples. Once harder material was found, the technique was changed to rotation drilling using a tricone with water injection system to recover grinded sediments. Sediment samples were collected from water overflowing the borehole. Samples were analyzed at macroscopic and microscopic levels in the lab to determine sediment composition and derive a stratigraphic cross section.

Electrical resistivity tomography (ERT) was applied at the cross section A–A to gain further insights into the subsurface structure. The ABEM Lund Imaging System (Dahlin 1996) was used with a Schlumberger array with a spacing of 5 m. This array consists of four collinear electrodes where the two inner electrodes are the receivers (potential) and the outter two are the current (source) electrodes. The potential electrodes remain fixed in position while succesive readings for increasig spacing of the source electrodes are taken (ASTM 1970). The ERT profile was 300 m long. The survey depth reached up to 60 m. The data inversion software used was RES2DINV (Loke and Barker 2004), and ERIGRAPH (Dahlin and Linderman 2007) was used for graphical presentation of 2D resistivity imaging.

Hydrogeologic Characterisation

Slug tests were performed for nine of the fifteen shallow piezometers. Slug tests are performed by adding or removing water instantaneously from the piezometer (Fetter 2001). Water level changes were measured with a Schlumberger DI501 mini diver (range of 10 m). Data analysis was performed using the method of Bouwer and Rice (1976) for unconfined aquifers and partially penetrating wells. Slug tests were also performed in the deeper piezometers specifically screened at different strata to estimate different hydraulic conductivity (K) values (P3W, P3E and P1W, P1E). Hydraulic conductivy describes the rate at which water can move through a permeable medium (Fetter 2001).

Groundwater levels were monitored continuosly in six piezometers (P1, P2, P3, P10, P11, P12) using Schlumberger mini divers. Data was recorded every 15 min from 21 of May through 30 July 2010. River level was also monitored at the A–A cross section. Barometric compensation of the data was performed using atmospheric pressure data recorded at the same interval and for the same period with a Schlumberger 50013, DI501 barometric diver (range of 1.5 m). Groundwater levels at the remaining piezometers and 21 shallow wells (depth 4.4 m to 11 m) were measured manually six times during the same period. Average groundwater levels from the shallow wells and shallow piezometers were used to derive the piezometric map.

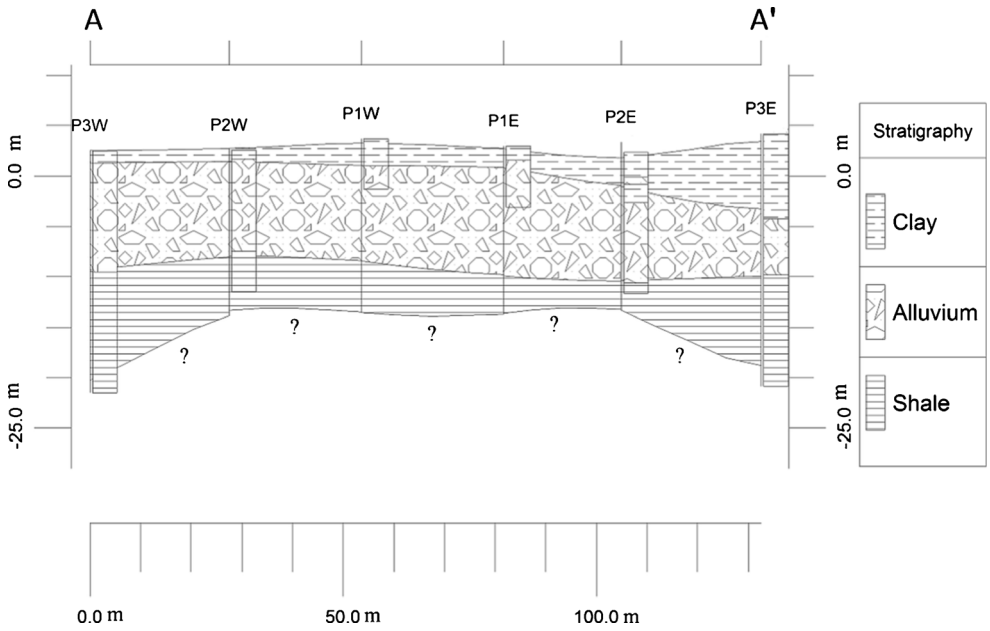

Fig. 2 Stratigraphic correlation in cross section A–A , vertical exaggeration 2X

Water Balance Estimation for the Dry Period

Precipitation was measured using a Tenite rain gauge. A Class A evaporation pan was installed at the same location (Fig. 1) to obtain daily evaporation measurements. Pan evaporation was corrected with an empirically derived pan coefficient depending on site specific conditions such as ground cover under the evaporation pan and type of crop surrounding the pan. The calculated evaporation also accounts for transpiration (Allen et al. 1998). In our case the coefficient was estimated at 0.7. Measurements of precipitation and evaporation were taken every morning.

The water balance was determined for the period between 21 May to 19 June 2010. Inflow terms included precipitation, groundwater inflow and surface water inflow, while outflow terms included evaporation, groundwater outflow, and surface water outflow. Groundwater extraction was considered negligible since there is only one pumping well, which was not functioning at the time.

Groundwater runoff was determined using the Darcy equation (Eq. 2)

$$Q = -KA\frac{dh}{dl} \tag{2}$$

where Q is runoff ($m^3\ d^{-1}$), K is hydraulic conductivity ($m\ d^{-1}$), A is cross sectional area (m^2); dh/dl is the hydraulic gradient (i), given by the hydraulic head difference between two points, dh (m) and the distance between those two points, dl (m).

Surface water inflow and outflow were set to zero for the period of study (dry season) as no flows could be detected. Groundwater storage changes were also considered. The water balance was estimated according to Eq. 3:

$$P + SW_{in} + GW_{in} = E + SW_{out} + GW_{out} + \frac{\Delta S}{\Delta t} \tag{3}$$

where P is precipitation ($m^3\ d^{-1}$), E is evaporation ($m^3\ d^{-1}$), SW is surface water runoff ($m^3\ d^{-1}$), GW is groundwater runoff ($m^3\ d^{-1}$), S is storage (m^3) and t is time (d).

Results

Coastal Geomorphology and Mangrove Forest Characteristics

The Ostional mangrove forest can be classified as riverine, occuring along the Ostional river estuary (Fig. 1). The geomorphology of this environment is determined by strong waves and littoral drift, which produces sand ridges along the coast. The mangrove forest is found behind these ridges, and it connects with the ocean trough the Ostional river outlet. During the study period, these ridges prevented direct surface connection between the mangrove and the sea; thus allowing surface water storage as backwater in the estuary (Online Resource 1).

Zonation patterns of three mangrove species were observed: red mangrove (*Rizophora mangle*) was found on the shore of the estuary with black mangrove (*Avicennia germinans*) further inland. Buttonwood *(Conocarpus erectus)* was found along the coast on higher beach ridges away from the tidal zone.

Soil Texture and Stratigraphy

All soil samples were classified as clay. Calculated cation exchange capacity (CEC) ranges between 25.95 meq 100 g-1 and 37.13 meq 100 g-1 .

Sediments collected during drilling on the East side of the river were composed of clay up to depths of 7 m. Samples reacted vigorously to HCl indic water runoff a ting high calcite content (Online Resource 2). Clay was in some cases mixed with subangular shale fragments (pebble size) like in P2E, probably the result of fluvial deposition. In the case of P1E and P3E, the clay layer was very homogenous. However,the clay deposits on the West side of the river were also combined with loam and shale fragments. Alluvial deposits were found beneath the clay layer. These were part of a heterogeneous layer composed of medium to fine sand, gravel and pebbles. The alluvium is thicker on the West side of the river, reaching 10 m thickness. Underneath the alluvium, a shale layer was found. Its thickness is unknown since perforations only reached 25 m depth. Although the drilling method did not allow the recovery of unaltered samples of this layer, inspection of an outcrop located 100 m to the north, showed a very high fracture density. Stratigraphic correlation along the cross section is shown in Fig. 2.

Comparison of stratigraphic correlation and the ERT profile (Fig. 3) shows a distintive resistivity for the shale layer relative to the upper alluvium and clay units. Saturated clay sediments showed resistivity values below 4.5 Ωm (black). Resistivity of dry clay and alluvial deposits range between 6.8 Ωm and 23 Ωm. A higher resistivity was observed on the upper part of P2E, where shale fragments where found. The shale showed resistivity values between 23 Ωm and 79 Ωm (light gray). The shale unit is observed as large outcrops at the coast (Online Resource 3). These observations may indicate that the shale unit pinches out towards the coast.

A slight resistivity difference was observed on the shale unit between west and east piezometers. Resistivity values were slighly lower on the west side, between 23 Ωm and 79 Ωm; whereas resistivity on the east side was above 79 Ωm. Drilling samples from west piezometers showed the same stratigraphy as east piezometers (Fig. 3). Since rotation drilling was used for the shale layer, no undisturbed samples could be recovered in order to determine if shale at this site had a greater fracture density. It could also be possible that there is a greater degree of saturation caused by water bearing fractures.

Hydrogeological System Analysis

Saturated Hydraulic Conductivity Hydraulic conductivity (K) values for each piezometer and averages for each strata are presented in Table 1. P3 had a K value of 13.37 m d^{-1} which could be caused by heterogeneities in the clay unit, thus it was not used to estimate the average value. Although average K values are very similar for all three strata, within the 10^{-2} m d^{-1} to 10 m d^{-1} range, the clay and alluvium strata were grouped into one aquifer unit and the shale into another. Since the number of K estimates is limited, we rely on additional evidence provided by the observation of high fracture density of the shale outcrops in the area to differentiate this unit from the others. Also, resistivity values show little contrast between the clay and alluvium, but a noticeable difference between these layers and the shale. Piezometric Surface of Shallow Aquifer and River StageGeneral groundwater flow direction is from NW to SE. The piezometric surface for the shallow aquifer is shown in Fig. 1. Groundwater depth varies between 0.5 m and 5 m. Groundwater levels in piezometers near the coast showed semidiurnal fluctuations due to the effect of sea tides (Fig. 4). P10 and P12 show a water level response to tidal effects due to pressure changes in the aquifer (Ferris et al. 1962). However, P11 (most distant from the sea) has a different behavior, responding mostly to precipitation events and showing small tide-induced fluctuations only when the water level is near or below 2 m. Hydraulic heads in piezometers next to the river (P3 and P1) showed an increase before 24 June 2010 and a sudden decrease on 25 June 2010, like the one observed in P11 (Fig. 4). The cause for this drop was the natural breakthrough of the river outlet due to increased water level caused by precipitation events. Once the system accumulated sufficient water, the

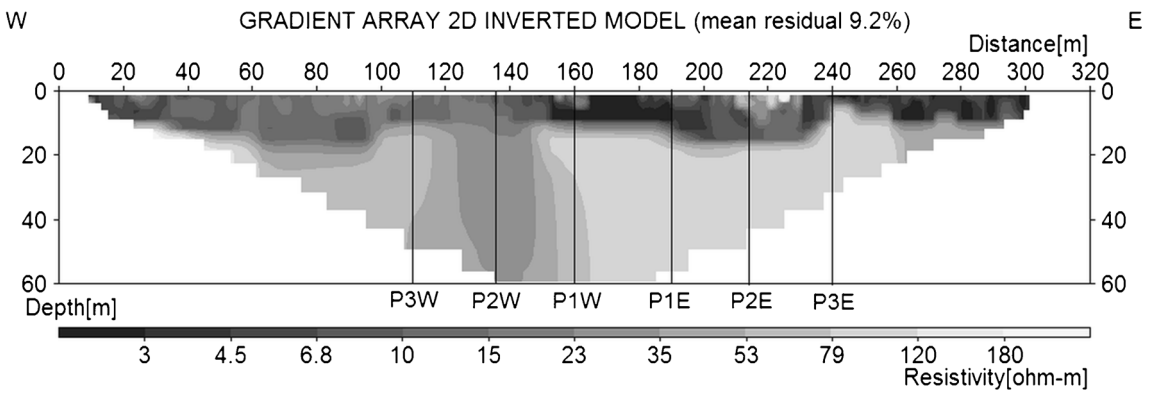

Fig. 3 ERT profile at the cross section A–A . Piezometer locations are also included

Table 1 Hydraulic conductivity estimates from slug tests, see Fig. 1 for locations

Stratum	Piezometer	K (m d^{-1})	Average K (m d^{-1})
Clay	P1	0.043	0.33
	P4	1.18	
	P5	0.23	
	P7	0.0006	
	P8	0.001	
	P10	0.88	
	P11	0.05	
	P12	0.29	
Alluvium	P1E	5.60	6.70
	P1W	7.80	
Shale	P3W	12.96	9.07
	P3E	5.18	

water level overtopped the beach ridges allowing direct surface discharge into the ocean, thus emptying the system and causing a rapid drop in hydraulic heads. Unfortunately, the river mini diver was stolen and surface water data could not be collected during this period.

Water Balance for the Shallow Aquifer

Average thickness for the shallow aquifer was estimated at 15 m based on the stratigraphy. The average width of the cross section was estimated at 500 m based on the limits of the mangrove forest (Fig. 1). Accumulated precipitation and evaporation were estimated to 145.8 mm and 99.8 mm for the 22 days of the study, respectively.

Table 2 summarizes the estimations of groundwater inflow and outflows. Hydraulic gradients (i) were estimated from the piezometric map (Fig. 1). Since the saturated zone is located mostly in the alluvium, we use its K estimate to calculate groundwater fluxes. The water balance estimates are shown is Table 3. Groundwater flow is the most uncertain estimation since we rely on average aquifer thickness from one cross section and few K estimates.

Table 2 Estimated groundwater inflow and outflow

	i (-)	K (m d^{-1})	Cross sectional area (m^2)	Q (m^3 d^{-1})
Groundwater in	0.002	6.7	7500	100.5
Groundwater out	0.003	6.7	7500	167.5

The positive storage term indicates an increase of about 1.7 mm d^{-1} in the mangrove area. The observed that average increase in the water table of shallow wells was 300 mm during a 30 day period.

Hydrochemistry

Ion concentrations and f_{sea} are presented in Table 4. The Piper diagram in Fig. 5 shows the freshwater (Ca–HCO_3) and seawater end-members (Na–Cl) along with all other samples. The first end-member is sample Wsw and the latter is sample Sea1. Salinization and refreshening processes are indicated too.

The anion triangle of the Piper diagram shows more clearly how samples are divided into three groups. Group 1 is closer to the freshwater end member and is composed of shallow wells. Group 2 is also composed of shallow wells (W15O, 17O and W4O) but with influence from grey water. Nitrate concentrations in the town wells vary between 0.0125 meq L^{-1} and 1.52 meq L^{-1} (Table 4). The highest value occurred at well W15O. Ammonium was not detected in any sample. Samples

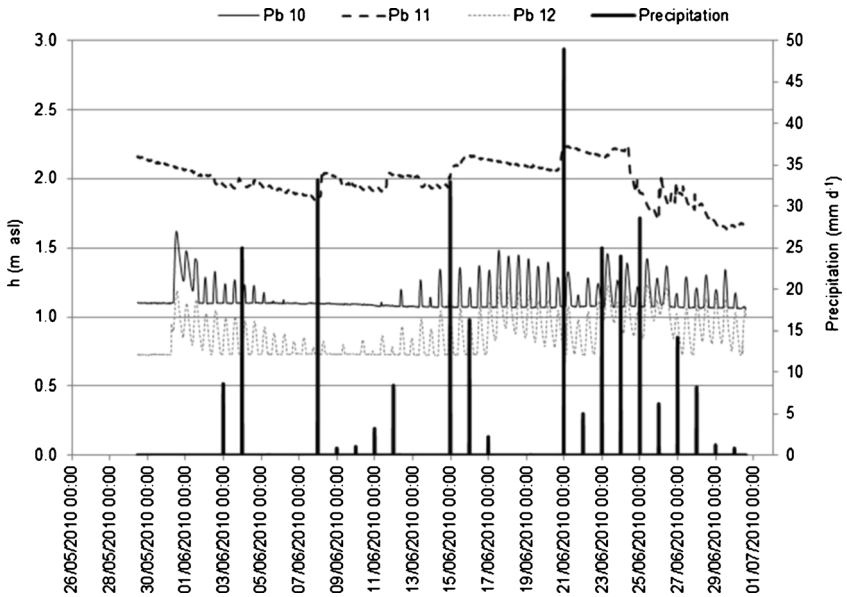

Fig. 4 Sea tide and precipitation effects in hydraulic heads in piezometers located near the coast. Pb10 and Pb12 depict stronger tidal influence due to more proximity to the shoreline, Pb11 is located further away and is more influenced by precipitation events

Table 3 Summary of the results for the water balance estimation for the period from 21 May to 19 June 2010

INPUT	Q (m^3 d^{-1})
Precipitation	1325.5
Groundwater	100.5
Surface water	0.0
Subtotal	1426.0
OUTPUT	Q (m^3 d^{-1})
Evaporation	907.3
Groundwater	167.5
Surface water	0.0
Subtotal	1074.8
Change in Storage	351.2

taken from the piezometers within the mangrove forest show concentrations of nitrate from 0 meq L^{-1} to 0.05 meq L^{-1}. However, P14 shows a distinctive higher nitrate value (0.1326 meq L^{-1}).

Group 3 is clearly more influenced by seawater and corresponds to river outlet samples and samples from piezometers located near to the coast or next to the river. The f_{sea} values for the third group varies between 0.04 and 0.4. Highest values correspond to piezometers near the coast. On the other hand, samples from shallow wells have f_{sea} between 0 and 0.02.

Relationships between major ions and Cl^- were also examined (Fig. 6). They were compared to the hypothetical mixing line between freshwater and seawater according to Appelo and Postma (1993) and Ghiglieri et al. (2012). In most cases, samples are grouped closer to the freshwater end-member on the hypothetical mixing line between freshwater and seawater. Only P14 and Sea2 are consistently in-between the two end members. Sample Sea2 was taken during low tide and although the Piper diagram classified it as Na–Cl facie, ionic correlation shows mixing with freshwater (Fig. 6a). Other piezometer and shallow well samples plot near the freshwater end member. However, P7 and P8 show depletion of Na^+ relative to Cl^- (Fig. 6a), and enrichment of Ca^{2+} (Fig. 6b), indicating salinitization, also shown in the Piper diagram. Whereas P4 and P5 show a slight enrichment in Na^+ which also confirms the refreshening process indicated in the Piper diagram (Fig. 5).

The relationship between Ca^{2+} and Cl^- is characterized by greater dispersion than in the pattern of other ionic correlations. Most of the samples plot above the mixing line, whereas the same samples plot below the mixing line for Na^+ and Cl^-. Additionally, the samples with higher f_{sea} (P7, P8, P4, P14 and Sea2) show a deficit in K^+ and Mg^{2+} (Fig. c and 6d).

Noticeable in Fig. 6e is the SO_4^{2-} concentration in P14 above the mixing line. Meanwhile, P11 which is also located within the mangrove forest and near the coast, plots very close to the freshwater end member. Other samples plot below the mixing line, indicating SO_4^{2-} depletion.

Table 4 Hydrochemistry results in meq L^{-1}, sample locations are shown in Fig. 1

Sample ID	Source	EC (µS cm^{-1})	pH (-)	T (°C)	Na^+	K^+	Mg^{2+}	Ca^{2+}	Mn^{2+}	Fe^{2+}	Cl^-	HCO_3^-	SO_4^{2-}	NO_3^-	f_{sea}
RU	SW	569	7.56	27.4	1.01	0.02	0.52	4.74	0.0011	0.0097	0.68	6.60	0.41	0.0077	0.00
*P*5	GW	2760	7.63	32.8	27.10	0.14	3.16	5.66	0.0660	0.0000	23.88	9.60	1.25	0.0004	0.04
*P*4	GW	4380	7.68	29.2	35.51	0.14	4.71	11.85	0.0888	0.0016	38.03	9.52	1.98	0.0000	0.07
*P*11	GW	3230	7.30	28.2	31.90	0.47	3.44	2.83	0.0252	0.0010	26.57	4.20	3.39	0.0509	0.05
Wsw	GW	629	7.57	27.6	1.01	0.01	0.30	5.12	0.0000	0.0000	0.72	6.60	0.19	0.0127	0.00
RO 1	SW	5000	7.61	31.5	46.33	0.69	9.26	5.36	0.0085	0.0000	46.02	6.20	4.75	0.0000	0.09
RO 2	SW	2220	7.74	28.9	15.00	0.29	3.55	5.19	0.0023	0.0014	16.39	6.80	1.89	0.0144	0.03
GrW	grey water	3050	6.97	28.5	31.12	1.33	1.39	5.90	0.0011	0.0000	16.28	18.00	8.31	0.0006	0.03
*P*14	GW	17230	7.60	28.1	199.71	2.13	34.64	16.42	0.0550	0.0022	204.84	16.40	42.23	0.1326	0.39
*P*7	GW	7660	7.31	28.1	62.75	0.62	13.07	16.82	0.1822	0.0005	75.46	11.12	4.74	0.0090	0.14
*P*8	GW	7230	7.47	28.9	39.00	0.66	17.53	27.62	0.5708	0.0003	64.18	6.96	4.96	0.0479	0.12
Sea1	sea	37400	7.60	31.3	460.74	7.40	99.98	15.86	0.0000	0.0003	519.08	2.44	49.99	0.0231	1.00
Sea2	sea	19800	7.36	29.6	217.97	2.09	41.34	8.96	0.0000	0.0000	244.43	4.80	23.16	0.0000	0.47
W15O	GW	2350	7.00	28.1	2.74	0.02	2.05	15.27	0.0001	0.0000	11.77	5.60	2.95	1.5183	0.02
W17O	GW	1386	7.04	28.9	2.12	0.02	1.41	11.21	0.0000	0.0000	6.48	5.20	1.55	0.2846	0.01
W2O	GW	755	7.35	28.1	2.23	0.03	1.03	4.35	0.0000	0.0000	1.86	5.00	0.65	0.0630	0.00
W4O	GW	1528	7.58	28.6	7.35	0.02	2.27	7.60	0.0000	0.0000	8.24	7.40	2.12	0.5037	0.01
W5O	GW	741	7.35	28.5	2.38	0.00	0.79	5.10	0.0000	0.0001	2.40	6.00	0.76	0.0237	0.00
W7O	GW	1015	7.42	28.7	2.72	0.02	0.81	7.26	0.0000	0.0006	2.93	7.80	1.20	0.2692	0.00
W8O	GW	1174	7.47	28.6	4.09	0.03	1.14	8.18	0.0004	0.0004	2.39	8.64	0.94	0.0604	0.00
W9O	GW	876	7.51	28.0	2.39	0.02	0.77	6.66	0.0000	0.0049	1.85	8.68	0.89	0.0125	0.00

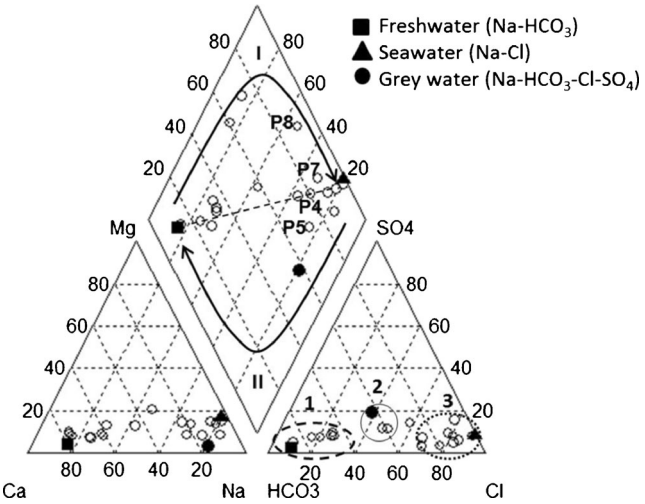

Fig. 5 Piper diagram, including freshwater and seawater endmembers, mixing line (dashed), salinization (I) and refreshening (II) processes. Circles in the anion triangle show freshwater samples (1), groundwater with grey water influence (2) and seawater influence (3)

Manganese was practically absent from shallow well samples and its concentration was very low in river water samples. Nevertheless, Mn^{2+} in piezometer samples within the mangrove forest reached concentrations up to 0.5708 meq L^{-1}. Iron was found at very low concentrations throughout the study area. Nonetheless, concentrations were at least one order of magnitude higher (10^{-3} meq L^{-1}) in piezometer samples than in shallow groundwater samples (10^{-4} meq L^{-1}).

Discussion

Beach Morphology and Water Balance

The most important source of freshwater during the study period was precipitation, despite high evaporation and groundwater discharge fluxes. Although the evaporation term includes transpiration, direct measurement of the mangrove forest transpiration flux may improve the calculation of the water balance. However, no substantial differences are expected since literature indicates that mangroves conserve water and thus transpiration rates are lower than non-saline plants (Lugo and Snedaker 1974; Saenger 2002).

Beach ridges (Fig. 7) are the main geomorphologic features in the study area that control freshwater and seawater mixing and in/outflows. Beach ridges are common on the Pacific Coast of Central America (Jimenez et al. 1999). Several authors describe beach ridges as essential geomorphological features of mangrove ecosystems (Thom 1967; Souza Filho and Paradella 2002; Jeanson et al. 2014); however, their role on the water balance dynamics of mangrove forests has not been studied in detailed. During low flow conditions, the ridges prevent river discharge into the ocean, causing flooding of the mangrove forest and groundwater and surface water accumulation. This is observed as increased groundwater levels. Water accumulation helps to maintain a positive water balance for the mangrove forest during dry periods. Sudden release of water occurs when accumulated water causes rupture of the beach ridges. This only happened once in the study period due to a larger precipitation event (Fig. 4).

The presence of beach ridges is crucial to guarantee sufficient freshwater availability within the mangrove forest, thus allowing its maintenance during dry periods. Other authors demonstrated that freshwater availability regulates growth, mortality, and phenological events. Changes in hydrological conditions would result in drastic alteration of structural and functional characteristics of the forest (Jimenez 1990; He et al. 2010).

A strong tidal influence was observed in head fluctuations of the coastal piezometers P10 and P12. In contrast, P11 was relatively unaffected by tides. Hydraulic head at Pb11 was around 2 m asl. Since average tidal fluctuation for the Pacific Ocean in Nicaragua is about 2 m (www.ineter.gob.ni), the response in P11 is damped when the head is above 2 m and becomes more evident when the head is below 2 m. Moreover, P11 was located furthest inland and had a f_{sea} of 0.05, which indicates lesser influence of the sea.

Hydrochemistry

Cationic exchange processes affected the chemistry of groundwater samples. Single freshwater-seawater mixing is not able to explain the Ca^{2+} enrichment and Na^{+} depletion shown in Fig. 6a and Fig. 6b. Calcite was found in thin sections from shale samples (Online Resource 2). Thus, groundwater mineralization is probably caused by calcite dissolution, as has been shown by other authors working in coastal aquifers (Giménez and Morell 1997; de Montety et al. 2008; Ghiglieri et al. 2012).

Coastal piezometers P11 and P14 show significant chemical differences. P11 showed a f_{sea} of 0.05 and its chemical composition resembles that of the freshwater end-member. Moreover, the groundwater level fuctuations show that P11 is not substantially affected by tides. P14 showed a f_{sea} of 0.39, indicating a strong seawater influence on its chemical composition. High concetrations of nitrate in P14 could be caused by inorganic nitrogen from tidal waters (Rivera-Monroy et al. 1995). In a study of hydrological and hydrogeochemical variations in the Itacurusa Experimental Forest in Brazil, nitrate concentrations peaked with high tide (Kjerfve et al. 1999). This is consistent with the the Na–Cl facie of this water sample. However, the SO_4^{2-} enrichment with respect to Cl^{-} in this sample cannot be explained merely by freshwater-seawater mixing.

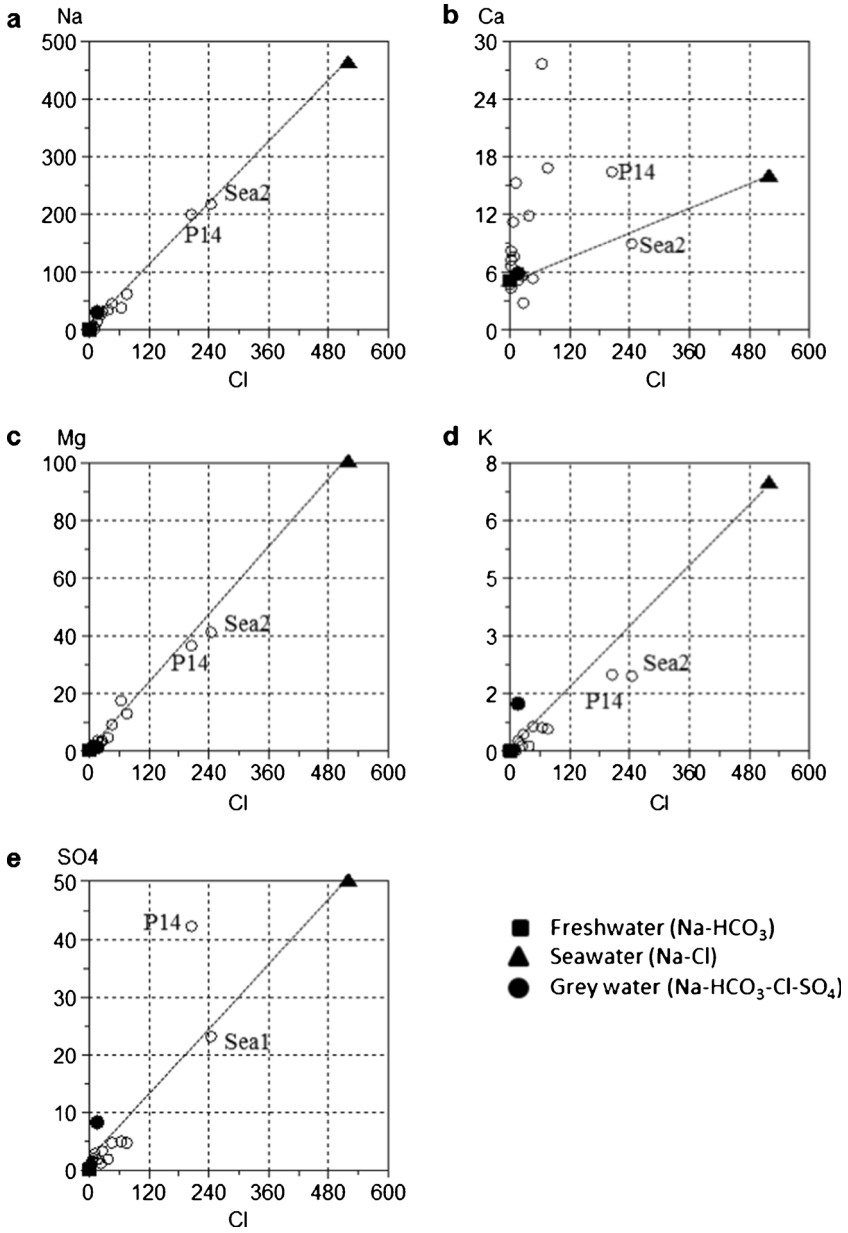

Fig. 6 Relationship between major ions and Cl⁻. All units in meq L^{-1}

Piezometers located on the west side of the river showed evidence of refreshening, whereas piezometers on the east side of the river indicated salinization. The deficit in Mg^{+} and K^{+} on the east side is further evidence of salinization process

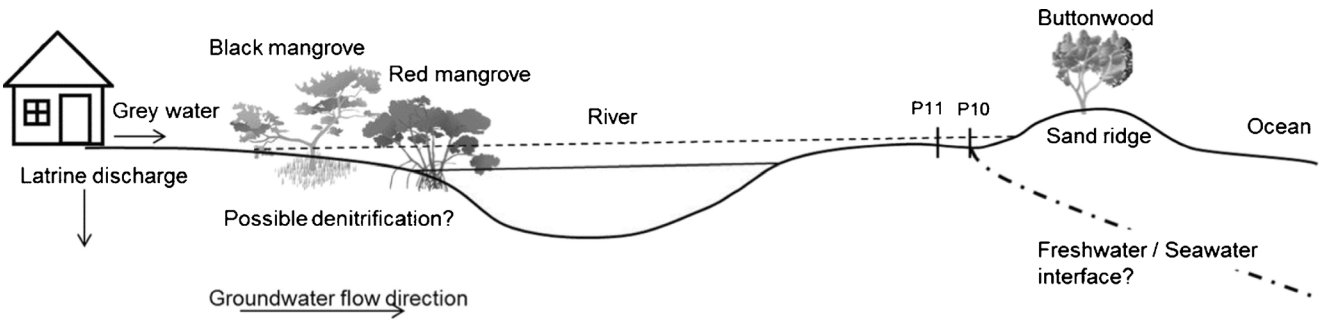

Fig. 7 Schematic cross-section of the study area, valid for area around cross section B–B . Dashed line indicates river flooding. For location see Fig. 1; not to scale. Mangrove tree images were taken from IAN/UMCES image library (http://ian.umces.edu/imagelibrary)

(Walraevens and Van Camp 2005). The clayish soils with high CEC provide the cation exchanger.

The hydrochemical difference between piezometers on the east side and west side of the river is the result of elevation differences and, thus, groundwater flow directions and fluxes. East side piezometers have a lower hydraulic head than west side piezometers and, consequently, receive more river water contributions.

The hydrochemistry of shallow wells in the town indicate influence of grey water infiltration. The most probable source of sodium and chloride in these wells are laundry and cleaning products (Fetter 1999), which are widely present in grey water. Grey water from households in Ostional is composed of laundry, shower, and kitchen waste waters. Sea water encroachment is ruled out due to the greater distance from the coast, the hydrochemcial evolution from the land towards the sea and the overall groundwater flow direction (towards the sea). Nitrate was also found in some wells (W170, W150 and W40), suggesting that their chemical composition is influenced by the proximity of latrines.

Presence of both Mn^{2+} and Fe^{2+} in piezometer samples within the mangrove forest may be evidence of occurrence of denitrification but further investigation is required to explore this possibility. Mangroves are recognized as nitrate sinks. Denitrification is usually slow in these environments (Rivera-Monroy and Twilley 1996; Alongi 2002), but rates can be increased through nitrate enrichment (Corredor and Morell 1994). Additionally, highly diverse and abundant microbial communities within mangrove sediments may catalyze the denitrification process (Corredor and Morell 1994).

Despite the negative connotation associated with the lack of a sewage treatment system in the study area, this could be also seen as an opportunity for the mangrove forest to receive extra nutrients inputs. Other authors have pointed out increases in denitrification rates (Corredor and Morell 1994) and in mangrove productivity with sewage inputs (Snedaker 1993). However, there is also evidence that nutrient enrichment by sewage can also negatively affect mangrove forests by rising mortality rates, increasing sensitivity to droughts, and affecting tree development due to heavy metal concentration in sewage. Additionally, eutrophication can cause an increase of the green house gas N_2O released by mangrove forests as an intermediate product of microbial denitrification and nitrification (Reef et al. 2010).

Conclusions

A detailed hydrological system analysis applying hydrological, hydrogeological and hydrochemical methods enabled gaining an in–depth understanding of the water balance dynamics in the mangrove forest during a dry season, which is critical to understand the forest subsistance. Precipitation events accounted for the most part of the freshwater input in the system. Net groundwater flux is negative. However, beach ridges along the coast prevent estuarine discharge into the ocean and facilitate storage of surface and groundwater in the mangrove ecosystem. The ridges break when large precipitation events occur, suddenly releasing accumulated water. Freshwater inputs maintain a positive water balance providing adequate conditions for mangrove growth and seedling survival during the dry period. The forest also receives extra nutrient inputs from the adjacent town. Groundwater mineralization occurs due to calcite dissolution but also due to seawater influence. Refreshening and salinization processes were identified on the west and east side of the river, respectively. These are determined by the general groundwater flow direction and the clayish soils provide the substrate for cationic exchange. Hydraulic and hydrochemical influence of seawater on groundwater is limited by the water table elevation at the coast and the amplitude of tidal fluctuations. These hydrological and geomorphological characteristics guarantee the continuation of the enviromental and socioeconomic services provided by this forest. Future research should focus on the investigation of nutrient inputs from the town and possible denitrifation processes within the mangrove forest.

Acknowledgments The authors wish to thank the National Autonomous University of Nicaragua (UNAN-Managua) and the Aquatic Resources Research Center (CIRA-UNAN) which granted the first author a study permit to conduct her PhD research. Funding was provided by the Dutch Fellowship Program from Nuffic (www.nuffic.nl) and the International Foundation for Science (IFS). Additionally, the first author's PhD studies were funded by the Faculty for the Future program (www.facultyforthefuture.net). Geophysical data collection and interpretation were performed in collaboration with Marvin Corriols, PhD fellow at Lund University, Sweden, and Lener Sequeira from the Geology and Geophysics Institute (IGG/CIGEO) at UNAN-Managua. Piezometer drilling was possible thanks to the support from Dr. Dionisio Rodriguez, Director of IGG/CIGEO and field technicians Francisco Vasquez and Walter Espinoza.

References

Alongi DM (2002) Present state and future of the world's mangrove forests. Environ Conserv 29:331–349

Allen RG, Pereira LS, Raes D, Smith M (1998) Crop evapotranspiration. Guidelines for computing crop water requirements-FAO Irrigation and drainage paper 56. FAO, Rome 300:6541

Appelo C, Postma D (1993) Geochemistry, groundwater and pollution. AA Balkema, Rotterdam

ASTM (1970) Special procedures for testing soil and rock for engineering purposes 5th edition. ASTM International, Maryland

Bouwer H, Rice R (1976) A slug test for determining hydraulic conductivity of unconfined aquifers with completely or partially penetrating wells. Water Resour Res 12:423–428

Briceño H, Miller G, Davis SE (2013) Relating freshwater flow with estuarine water quality in the Southern Everglades mangrove ecotone. Wetlands. doi:10.1007/s13157-013-0430-0:1-11

Cahoon DR, Hensel P, Rybczyk J, McKee KL, Proffitt CE, Perez BC (2003) Mass tree mortality leads to mangrove peat collapse at Bay Islands, Honduras after Hurricane Mitch. J Ecol 91:1093–1105

Carvalho F, Montenegro-Guillen S, Villeneuve JP, Cattini C, Bartocci J, Lacayo M, Cruz A (1999) Chlorinated hydrocarbons in coastal lagoons of the Pacific coast of Nicaragua. Arch Environ Contam Toxicol 36:132–139

Castañeda-Moya E, Rivera-Monroy VH, Twilley RR (2006) Mangrove zonation in the dry life zone of the Gulf of Fonseca, Honduras. Estuar Coasts 29:751–764

CBM (2002) El Corredor Biológico Mesoamericano: Una plataforma para el desarrollo sostenible regional (The Mesoamerican Biological Corridor: a platform for regional sustainable development). Proyecto Corredor biológico mesoamericano

CIRA (2008) Disponibilidad actual y futura de los recursos hídricos en la franja costera del municipio de San Juan del Sur (Actual and future water resources availability in the coastal area of the municipality of San Juan del Sur). Centro para la Investigación en Recursos Acuáticos de Nicaragua, Managua, p 103

Corredor JE, Morell JM (1994) Nitrate depuration of secondary sewage effluents in mangrove sediments. Estuar Coasts 17:295–300

Dahlin T (1996) 2D resistivity surveying for environmental and engineering applications. First Break 14:275–283

Dahlin T, Linderman JE (2007) Software Developed in Cooperation between ABEM. Lund University and Terraohm

de Montety V, Radakovitch O, Vallet-Coulomb C, Blavoux B, Hermitte D, Valles V (2008) Origin of groundwater salinity and hydrogeochemical processes in a confined coastal aquifer: Case of the Rhône delta (Southern France). Appl Geochem 23:2337–2349

Ellison A (2004) Wetlands of Central America. Wetl Ecol Manag 12:3–55

Feller IC, Sitnik M (1996) Mangrove ecology workshop manual. Smithsonian Institution, Washington, DC:135

Ferris JG, Knowles D, Brown R, Stallman RW (1962) Theory of aquifer tests. US Geological Survey

Fetter C (2001) Applied hydrogeology 4th edition. Prentice Hall Upper Saddle River, New Jersey

Fetter CW (1999) Contaminant hydrogeology. Prentice Hall Upper Saddle River, New Jersey

Fürst E, Barton DN, Jimenez G (2000) Partial economic valuation of mangroves in Nicaragua In McCracken, JR and Abaza, H (eds.) Environmental valuation: a worldwide compendium of case studies, edn. Earthscan, UK, p 233

Ghiglieri G, Carletti A, Pittalis D (2012) Analysis of salinization processes in the coastal carbonate aquifer of Porto Torres (NW Sardinia, Italy). J Hydrol 432–433:43–51

Gilman EL, Ellison J, Duke NC, Field C (2008) Threats to mangroves from climate change and adaptation options: a review. Aquat Bot 89: 237–250

Giménez E, Morell I (1997) Hydrogeochemical analysis of salinization processes in the coastal aquifer of Oropesa (Castellón, Spain). Environ Geol 29:118–131

Gondwe BN, Hong S-H, Wdowinski S, Bauer-Gottwein P (2010) Hydrologic dynamics of the ground-water-dependent Sian Ka'an wetlands, Mexico, derived from InSAR and SAR data. Wetlands 30:1–13

Groombridge B (1992) Global biodiversity: status of the earth's living resources. Chapman & Hall

Gross J, Flores E, Schwendenmann L (2013) Stand structure and aboveground biomass of a *Pelliciera rhizophorae* mangrove forest, Gulf of Monitjo Ramsar site, Pacific Coast. Panama Wet lands. doi:10.1007/s13157-013-0482-1:1-11

He G, Engel V, Leonard L, Croft A, Childers D, Laas M, Deng Y, Solo-Gabriele H (2010) Factors Controlling Surface Water Flow in a Low-gradient Subtropical Wetland. Wetlands 30:275–286

Jeanson M, Anthony E, Dolique F, Cremades C (2014) Mangrove Evolution in Mayotte Island, Indian Ocean: A 60-year Synopsis Based on Aerial Photographs. Wetlands. doi:10.1007/s13157-014-0512-7:1-10

Jimenez J (1990) The structure and function of dry weather mangroves on the Pacific Coast of Central America, with emphasis on *Avicennia bicolor* forests. Estuaries 13:182–192

Jimenez J (1992) Mangrove forests of the Pacific coast of Central America. Coastal plant communities of Latin America:259-267

Jimenez J, Yañez-Arancibia A, Lara-Domínguez A (1999) Ambiente, distribución y características estructurales en los manglares del Pacífico de Centro América: contrastes climáticos (Environment, distribution and structural characteristics of mangrove forests in Central America: climatic contrasts). In Yañez-Arancibia, A and Lara-Domínguez, A (eds.) Ecosistemas de manglar en América Tropical, 1st edn. Instituto de Ecología, A.C. Centro SEP - CONACYT, Mexico, pp 51-70

Keddy PA (2010) Wetland ecology: principles and conservation Second edition. Cambridge University Press, UK

Kjerfve B, Lacerda L, Rezende CE, Ovalle ARC (1999) Hydrological and hydrogeochemical variations in mangrove ecosystems. In Yañez-Arancibia, A and Lara-Domínguez, A (eds.) Mangrove ecosystems in tropical America: structure, function and management, 1st edn. Instituto de Ecología, A.C. Centro SEP - CONACYT, Mexico, pp 71-81

Krasny J, Hecht G (1998) Estudios hidrogeológicos e hidroquímicos de la Región del Pacífico de Nicaragua (Hydrogeologic and hydrochemical studies of the Pacific Region of Nicaragua). INETER, Managua, p 154

Loke M, Barker R (2004) RES2Dinv software. Geotomo Software Company

Lovelock C, Feller IC, McKee K, Ball M (2004) The effect of nutrient enrichment on growth, photosynthesis and hydraulic conductance of dwarf mangroves in Panama. Funct Ecol 18:25–33

Lugo AE, Snedaker SC (1974) The ecology of mangroves. Annu Rev Ecol Syst 5:39–64

Magaña V, Amador JA, Medina S (1999) The midsummer drought over Mexico and Central America. J Clim 12:1577–1588

McClain ME, Subalusky AL, Anderson EP, Dessu SB, Melesse AM, Ndomba PM, Mtamba JOD, Tamatamah RA, Mligo C (2013) Comparing flow regime, channel hydraulics and biological communities to infer flow-ecology relationships in the Mara River of Kenya and Tanzania. Hydrol Sci J. doi:10.1080/02626667.2013.853121

Perez M, Siria I, Sotelo M, Robleto R (2008) Estudio de pre-factibilidad sobre produccion y comercialización de *Anadara tuberculosa* y *Anadara similis* en los manglares del municipio de Tola, Rivas (Pre-factibility study on the production and comercialization of *Anadara tuberculosa* and *Anadara similis* in the Tola Mangroves, Rivas). GTZ, Managua, p 55

Polidoro BA, Carpenter KE, Collins L, Duke NC, Ellison AM, Ellison JC, Farnsworth EJ, Fernando ES, Kathiresan K, Koedam NE (2010) The loss of species: mangrove extinction risk and geographic areas of global concern. PLoS One 5:e10095

Pool DJ, Snedaker SC, Lugo AE (1977) Structure of mangrove forests in Florida, Puerto Rico, Mexico, and Costa Rica. Biotropica:195-212

Rabinowitz D (1978) Early growth of mangrove seedlings in Panama, and an hypothesis concerning the relationship of dispersal and zonation. Journal of Biogeography:113-133

Reef R, Feller IC, Lovelock CE (2010) Nutrition of mangroves. Tree Physiol 30:1148–1160

Rivera-Monroy V, Twilley R, Boustany R, Day J, Veraherrera F, Ramirez M (1995) Direct denitrification of mangorve sediments in terminos Lagoon, Mexico. Mar Ecol Prog Ser 126:97–109

Roth LC (1992) Hurricanes and mangrove regeneration: effects of Hurricane Joan, October 1988, on the vegetation of Isla del Venado, Bluefields, Nicaragua. Biotropica:375-384

Saenger P (2002) Mangrove ecology, silviculture and conservation. Springer Netherlands

Schumacher M (2007) Formulación e implementación de medidas de conservación de manglares (Design and implementation of conservation actions for mangrove forests). GTZ, Managua, p 51

Sherman RE, Fahey TJ, Howarth RW (1998) Soil-plant interactions in a neotropical mangrove forest: iron, phosphorus and sulfur dynamics. Oecologia 115:553–563

SINAPRED (2005) Plan de gestion de riesgos. Departamento de Rivas. Municipio de San Juan del Sur. (Risk management plan. Rivas Department. Municipality of San Juan del Sur). pp 102

Smith AP, Hogan KP, Idol JR (1992) Spatial and temporal patterns of light and canopy structure in a lowland tropical moist forest. Biotropica:503-511

Snedaker SC (1993) Impact on mangroves. In Maul, GA (ed.) Climatic change in the Intra-American Seas: implication of future climate change on the ecosystems and socio-economic structure of the marine regimes of the Caribbean Sea, Gulf of Mexico, Bahamas and NE Coast of S. America, 1st edn., London, pp 282-305

Souza Filho PWM, Pardella WR (2002) Recognition of the main geobotanical features along the Bragança mangrove coast (Brazilian Amazon Region) from Landsat TM and RADARSAT-1 data. Wetl Ecol Manag 10:121–130

Spalding M, Blasco F, Field CD (1997) World mangrove atlas. Earthscan, UK

Swain F (1966) Bottom sediments of lake Nicaragua and lake Managua, Western Nicaragua. J Sediment Res 36:522–540

Thom BG (1967) Mangrove ecology and deltaic geomorphology: Tabasco, Mexico. The Journal of Ecology 55:301–343

UNA (2003) Actualización del estado del recurso suelo y capacidad de uso de la tierra del municipio de San Juan del Sur. Universidad Nacional Agraria, Managua, p 44

Walraevens K, Van Camp M (2005) Advances in understanding natural groundwater quality controls in coastal aquifers. In Araguas, L, Custodio, E and Manzano, M (eds.) Groundwater and Saline Intrusion. Selected papers from the 18th SWIM meeting., 1st edn. IGGM, Madrid, pp 449-463

Weeda R (2011) Hydrogeobiochemistry in a small tropical delta. Master thesis, Vrije Universiteit, Amsterdam